Local Legendre Polynomial Fitting-Based Preprocessing for Improving the Interpretation of Permutation Entropy in Stationary Time Series

Meryem JABLOUN
Orleans University, PRISME laboratory 12 rue de Blois, 45000 Orleans, France.

***Abstract*—Permutation entropy (PE) and its variants are ordinal pattern-based techniques that have become widely used as complexity measures to quantify the degree of disorder or randomness in a time series. Despite their popularity, these techniques have several limitations, such as sensitivity to the embedding dimension, the sampling frequency, and their specific preprocessing strategies. The information captured by these techniques is difficult to interpret and may not fully reflect the complexity of time series.**

We propose an alternative PE variant to overcome these limitations. We first divide the signal into short segments of a fixed length sufficient enough to allow for a local polynomial modelling of this signal. We use a discrete orthonormal polynomial basis of a limited degree to ensure that for each segment, the model parameters obtained are uncoupled and have similar value ranges. By ranking these parameters, we construct an ordinal pattern (OP) for each segment. The proposed PE variant is then defined as the Shannon entropy applied to the probability distribution of these OPs.

The proposed local polynomial fitting-based preprocessing helps improve the PE interpretation. The advantages of the proposed PE method over some existing PE variants are demonstrated using simulated signals and real data.

***Index Terms*—Legendre polynomial modelling, multiscale permutation entropy, stationary process.**

I. Introduction

Measuring the complexity of time series is an important signal processing task that is useful in a variety of applications, including prediction, anomaly detection, classification, and signal processing analysis [1]–[6]. The complexity measure helps provide valuable insights into the structure and dynamics of the systems that generate the data.

In particular, the permutation entropy (PE) was introduced in [7] as a natural complexity measure of time series. The basic idea behind the PE is to convert the time series into a symbolic sequence, the symbols are the relative ranks of d consecutive sample values and they are called ordinal patterns (OP) of order d. The PE is then defined as the Shannon entropy applied to the probability distribution of these OPs.

PE has gained increasing attention over the last two decades, and several PE variants have been proposed in the literature to address specific challenges and requirements in various applications. One such example is the multiscale permutation entropy (MPE). Some of MPE based-methods can be considered as linear preprocessing-based techniques that combine, on the one hand, delay operators, linear filtering, and subsampling to uncover hidden signal structures and, on the other hand, different estimation strategy of PE [8]–[15]. However, these MPE are very sensitive to the sampling frequency and they are prone to aliasing phenomenon at large scales [16]–[18].

Other MPE methods are nonlinear preprocessing techniques that combine data-driven signal decomposition and PE estimators. It has been demonstrated in [19] that these MPE methods primarily reflect the shift in the mean frequency of the signal spectra. Both linear and nonlinear preprocessing-based MPE methods do not take into account the growth rate of the signal. As a result, a unique symbol is assigned to different sample sequences with varying growth rates. Unlike the previously cited MPE methods, the amplitude-aware PE proposed in [20], [21] takes into account the growth rate of the signal, while the phase PE proposed in [22] considers the phase patterns obtained using the Hilbert transform of the signal. However, the latter two MPE methods are very sensitive to noise.

Developing alternative PE measures is still necessary to overcome the limitations of PE and MPE. In this paper, we propose a new variant of MPE, named the local Legendre polynomial modeling-based permutation entropy (LPPE). The main concept is to locally model the signal using an orthonormal polynomial basis of limited degree $d-1$. To this end, the signal is first divided into short segments of fixed length L, where $L \geq d$. For each segment, we estimate d parameters of the local signal model using a least-squares approach. These parameters are then ranked to form the OP of length d. The Shannon entropy is finally calculated using the probability distribution of the obtained OPs.
We use the well-known Legendre polynomials to create an orthonormal polynomial basis. The orthonormality property ensures uncoupled parameters with similar value ranges and allows for a reliable ranking procedure. These parameters implicitly provide information about the growth rate, concavity, etc., which helps better characterize and interpret the PE measure of the signal. The proposed LPPE method outperforms classical MPE in terms of robustness to noise thanks to the use of L samples to produce the OP of length d.

The paper is organized as follows. Section II recalls the PE and MPE concepts and their limitations. The proposed LPPE is detailed in Section III. Section IV presents simulations and real data processing to illustrate the potential of the proposed method. Finally, Section V concludes this work.

II. Theoretical background

This section provides an overview of the PE and MPE and highlights their limitations through illustrative examples.

A. PE and MPE concepts

Let us consider a discrete-time signal x_t and use an ordinal methodology to convert it into a sequence of symbols called OPs. For example, an OP of order d can be obtained by ranking d adjacent values $x_t, x_{t+1}, \ldots, x_{t+d-1}$ in ascending order. For instance, the unique OP '2413' of length $d=4$ is assigned to the four consecutive samples $1.1, 2.3, -0.3, 1.2$, whereas two consecutive OPs '231' and '312' of length d=3 are assigned to these same samples. And for $d=2$, these samples are coded by 3 consecutive OPs '12', '21' and'12'.

Note that this ordinal methodology does not consider the growth rate of the signal, which can result in different sample sequences with varying growth rates being assigned the same OP. For instance, when $d=3$, the OP '123' would be assigned to both the sequences $0.01, 0.02, 0.03$ and $0.01, 4.02, 40.03$.

The occurrence of OP of type Π_i can be estimated, subject to a sample number N very high compared to d, as follows:

$$p_{\Pi_i} = \left\{ \frac{\#t \ | \{x_t, x_{t+1}, \ldots, x_{t+d-1}\} \text{ of type } \Pi_i}{N-d+1} \right\}, \quad (1)$$

where $\#$ denotes the cardinal. The PE of order d, as introduced in [7] for weakly stationary signals, is defined as the Shannon entropy applied to the probability distribution of OPs (1):

$$H = -\sum_i p_{\Pi_i} \log(p_{\Pi_i}). \quad (2)$$

In theory, there are $d!$ possible distinct OPs of order d regardless of the ordering methodology. This assumes that equal values are infrequent. As a result, the normalized PE can be utilized instead of (2):

$$H = -\frac{\sum_i p_{\Pi_i} \log(p_{\Pi_i})}{\log(d!)}. \quad (3)$$

Several MPEs have been proposed in the literature to examine multi-scale aspects. Most of MPE are variants of PE in which the input signal is modified through preprocessing techniques such as linear filtering, delay operators, subsampling, or data-driven decomposition. Due to lack of space, readers may refer to [8]–[15] for more details. For comparison purposes, we only remind that the coarse-grained MPE method [8] uses a moving average filter of order M, followed by subsampling with a factor M. The value of M is referred to as the scale.

B. PE and MPE limitations

The main limitations of PE and MPE can be succinctly stated as follows. Sensitivity to the embedding dimension (OP order) d: Small values of d may not adequately capture the signal complexity, leading to misinterpretation of the analysis results. On the opposite, large values of d increase the computational cost, especially when dealing with large or high-dimensional signal. Bias estimation for finite-length time series: According to [13], [23], a large sample size is necessary to reduce bias in the estimation process. In addition, the constraint $\frac{N}{M} \gg d$ should be satisfied in order to ensure accurate results. Impact of noise and sampling frequency: Both PE and MPE are sensitive to noise and the sampling frequency, as reported in [16], [18]. The sampling frequency can significantly alter the OP distribution, particularly when it is close to Nyquist rate [24]. At high sampling frequencies, even low-level noise can have a significant impact on the OP distribution. Additionally, at larger scales, MPEs are susceptible to the aliasing caused by subsampling step.

The limitations of PE and MPE can be illustrated by examining two examples of well-structured signals.

a) 1^{st} signal: x_t=$\sin(2\pi\nu_0 t + \phi)$ where ϕ is a random phase that follows an iid uniform distribution on $[-\pi, \pi[$ and ν_0 is the reduced frequency. Figure 1 displays the mean PE (3) using 100 Monte Carlo realizations of x_t for each $\nu_0 \in]0.25, 0.5[$. The sample size is $N = \lfloor 10^3 \nu_0^{-1} \rfloor$.

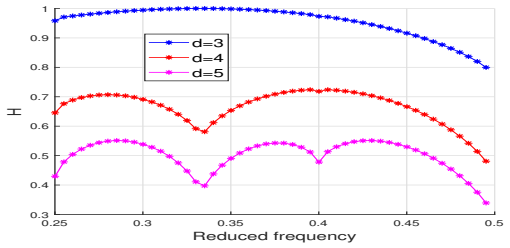

Fig. 1: Mean PE (3) of $x_t = \sin(2\pi\nu_0 t + \phi)$ where ϕ is an iid uniform random variable distributed on $[-\pi, \pi[$. 100 Monte Carlo realizations of 1000 periods of x_t were generated for each $\nu_0 \in]0.25, 0.5]$.

For example, for ν_0=0.41 and d=3, the mean PE is found to be 0.967. This value is comparable to that of a slightly correlated random Gaussian process [25], making it difficult for PE to differentiate between the two processes. The mean PE decreases to 0.722 when the OP order is set to d=4, and further decreases to 0.529 when the order is increased to d=5. However, a higher order $d \geq 6$ results in a poor estimation of the OP occurrence (1), we remind that $d!$>720 OPs are possible in this case and the sample size is N=2439. Furthermore, all linear preprocessing-based MPEs [8]–[15] cannot be used as no scale can avoid aliasing induced by subsampling. Similarly, data-driven decomposition-based MPEs are ineffective as only one component can be identified. In addition, if x_t is degraded by high-level noise, MPE methods described in [20]–[22] fail to distinguish between uncorrelated random noise and this sinusoidal process for d=3. These observations remain valid for deterministic sinusoidal signals [18].

b) 2^{nd} signal: $y_t = \sin(2\pi 0.41t) + \sin(2\pi 0.31t) + \sin(2\pi 0.21t)$ with a sample size N=2439; the PEs of order d=3 and d=4 are found to be 0.993 and 0.973, respectively. The PE decreased to 0.870 for d=5. Higher order OPs still have poor significance and previously published MPEs are still not suitable for measuring this signal complexity.

In the following, we propose a new variant of MPE that aims to better capture the complexity of time series.

III. Proposed MPE: LPPE

Let's consider a discrete time series x_t with t=0, 1, . . . , N−1. We divide this signal into short segments of fixed length L: the i^{th} segment is $[x_i, x_{i+1}, \ldots, x_{i+L-1}]$. According to Weierstrass's theorem, a polynomial approximation of the signal can be locally performed on each segment i:

$$x_t = \sum_{n=0}^{d-1} a_{i,n} P_n(t-i) + \epsilon_t \text{ for } t = i, i+1, \ldots, i+L-1, \quad (4)$$

where $P_n(t)$ is a polynomial of degree n and ϵ_t is the approximation error. The segment length L is chosen to ensure local stationarity and is kept small enough to allow for a limited degree of polynomial modeling $d-1$ with $(d \leq L)$. We use a discrete orthonormal polynomial basis, $P_n(t)$ with $n = 0, 1, \ldots, d-1$, created using the well-known Legendre polynomials.

The d model parameters on segment i are denoted by $a_{i,n}$ and are estimated using a local least squares (LS) strategy:

$$\hat{a}_{i,0}, \hat{a}_{i,1}, \ldots, \hat{a}_{i,d-1} = \underset{a_{i,0}, a_{i,1}, \ldots, a_{i,d-1}}{\arg\min} \sum_{t=i}^{i+L-1} \left| x_t - \sum_{n=0}^{d-1} a_{i,n} P_n(t-i) \right|^2. \quad (5)$$

The LS estimation strategy is equivalent to the maximum likelihood one if assuming ϵ_t to be a white Gaussian with unknown variance ${\sigma_\epsilon}^2$. The Fisher information matrix can be then calculated to be ${\sigma_\epsilon}^{-2} I$, with I being the identity matrix of size $d \times d$. This guarantees uncoupled model parameters. These estimated parameters (5) are then ranked to build the ordinal pattern Π. This ordinal methodology ensures that the signal growth rate and concavity are taken into account. The proposed LPPE is then defined using equation (3) and:

$$p_{\Pi_i} = \left\{ \frac{\#t \mid \{a_{t,0}, a_{t,1}, \ldots, a_{t,d-1}\} \text{ of type } \Pi_i}{N - L + 1} \right\}. \quad (6)$$

By varying L and d under the constraint $L \ll N$ and $d \leq L$, we explore the multiscale aspect of the proposed LPPE. The orthonormality property ensures uncoupled parameters with similar value ranges and thus a reliable ranking procedure. The model parameters (4) are implicitly linked to the first d higher-order derivatives of the signal, such as the local growth rate (first derivative), local convexity/concavity (second derivative), and so on. This helps to better characterize and interpret the PE-based complexity measure of the signal. Furthermore, the proposed LPPE takes advantage of L consecutive samples to generate the OP of order d, unlike classical MPEs which use only d samples. This enhances robustness to fluctuations and noise. Additionally, the proposed LPPE does not require subsampling, thereby avoiding aliasing problems.

IV. Results

This section focuses on the performance study of the proposed LPPE. Simulated signals and real data are processed using the proposed LPPE and compared to the classical PE and MPE [7].

A. Uncorrelated versus correlated Gaussian processes

Consider three Gaussian processes: white Gaussian noise (WGN) with zero mean and unit variance, and two autoregressive processes (AR1 and AR2) of orders 51 and 26, respectively. The frequency responses of these two AR processes (with 3 dB bandwidths of 0.035 and 0.08) are depicted in fig.2a and 2c, respectively. Both AR processes are centered at the same reduced frequency of 0.225. The mean of the proposed LPPE (6) (3) of orders $d = 3, 4$, and 5 is shown in fig.2b, 2d, and 2f, based on 100 Monte Carlo simulations, the sample size being $N = 10^4$. Only the mean of the classical PE (1) (3) is shown with a solid circle marker, as classical MPEs with scale $M \geq 2$ lead to aliasing in the case of AR2.

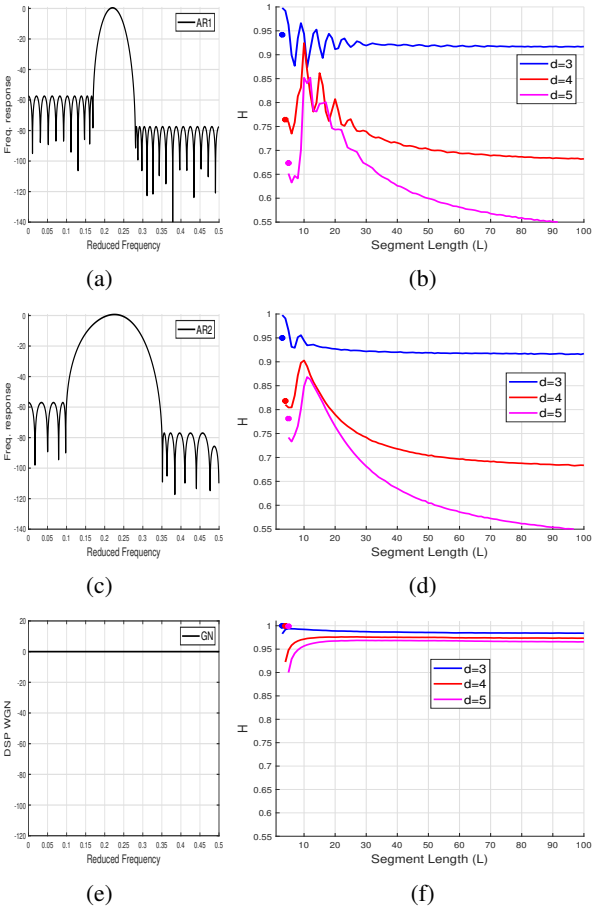

Fig. 2: LPPE of Gaussian processes: (a) and (c) frequency responses of AR1 and AR2 filters, respectively. (e) power spectral density (PSD) of WGN. Mean LPPE (6) (3) (solid line) of orders d= 3, 4, and 5 as a function of L for (b) AR1 process, (d) AR2 process and (f) WGN. (Solid circle marker) classical PE (1) (3) with same d values. All curves are based on 100 Monte Carlo simulations and N=10^4.

Figure 2f shows that for WGN, the proposed LPPE is consistently higher than 0.9, regardless of the value of d, and it is free of oscillations regardless of the segment length L. As L increases above 11, the LPPE converges towards stable

and close values of 0.984, 0.974, and 0.967 for $d = 3, 4$, and 5, respectively. On the other hand, for correlated processes AR1 and AR2 (fig.2b and 2d), the LPPE falls below 0.90 and decreases as L increases above 11, reaching a low but distinct values of 0.683 and 0.55 for $d = 4$ and 5, respectively. For both AR processes, the LPPE with $L > 30$ and $d \geq 4$ is better at distinguishing these models from WGN, compared to the classical PE represented by a solid circle marker. Moreover, AR1 process exhibits more noticeable oscillations than AR2, primarily due to its smaller bandwidth size. This point will be clarified in the next paragraph on narrower bandwidth signals.

B. Sinusoidal signals

Single and multicomponent sinusoidal signals with iid random phases uniformly distributed on $[-\pi, \pi[$ are considered. All curves are based on 100 Monte Carlo simulations.

We first analyze the stationary random process $x_t = \sin(2\pi\nu_0 t + \phi)$ from section III. Figures 3a, 3b, and 3c display the proposed LPPE for $\nu_0 = 0.205$, 0.41, and 0.33, respectively. The sample size for each figure is $N{=}\lfloor 10^3 \nu_0^{-1} \rfloor$. Remind that the classical PE for $\nu_0 = 0.41$ can be equivalent to some MPE variants [8], [10], [15] for $\nu_0 = 0.205$ obtained with a scale of $M = 2$.

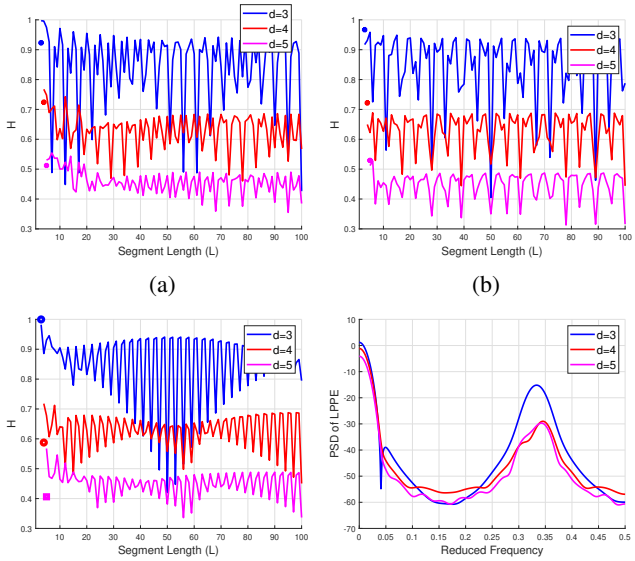

(a) (b) (c) (d)

Fig. 3: LPPE of $x_t = \sin(2\pi\nu_0 t + \phi)$ evaluated using 100 Monte Carlo simulations of random phase ϕ. 1000 periods are generated. (a), (b) and (c) Mean LPPE using d=3, 4 and 5 for $\nu_0{=}0.205, 0.41$ and 0.33, respectively. (Solid circle marker) classical PE with same d values. (d) PSD of mean LPPE for $\nu_0{=}0.33$.

As can be seen from Fig.3, the LPPE for a pure tone signal is an oscillating function of $L \geq \nu_0^{-1}$, and it appears to reach very low values, below 0.5, when $L\nu_0 \in \mathbb{N}$. Similar observations (see fig.4) can be made when considering a multicomponent signal with random phases: $y_t = \sin(2\pi 0.41t + \phi_0) + \sin(2\pi 0.31t + \phi_1) + \sin(2\pi 0.21t + \phi_2)$ and a sample size $N{=}\lfloor 10^3 0.21^{-1} \rfloor$.

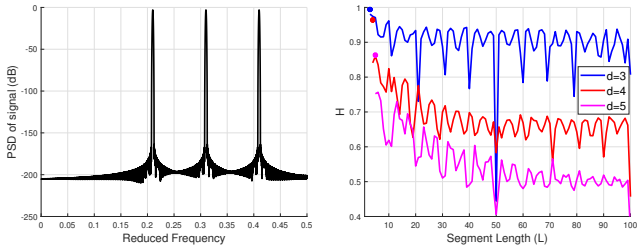

(a) (b)

Fig. 4: LPPE applied to an example of multicomponent sinusoidal signals: (a) PSD of the signal and (b) Mean LPPE using d=3,4 and 5.

C. Sinusoidal signals embedded in noise

We here consider a sinusoidal signal $x_t{=}\sin(2\pi\nu_0 t)$ with $\nu_0 = 0.205$ embedded in additive WGN, the sample size is $N{=}\lfloor 10^3 \nu_0^{-1} \rfloor$. Figure 5 shows the LPPE obtained at different signal to noise ratios (SNR). As can be seen from fig.5, the LPPE increases but still oscillating even for low level noise which distinguishes it from the LPPE of WGN.

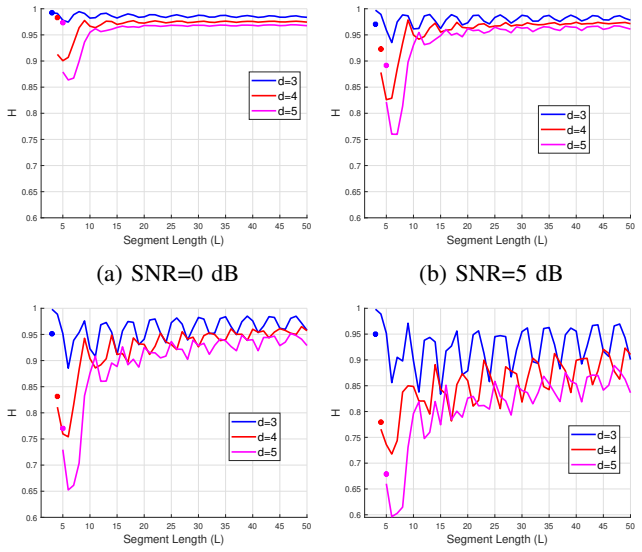

(a) SNR=0 dB (b) SNR=5 dB

(c) SNR=10 dB (d) SNR=15 dB

Fig. 5: Mean LPPE of a pure tone sinusoidal ($\nu_0 = 0.205$) embedded in an additive WGN obtained using d=3,4 and 5. All curves are based 100 Monte Carlo simulations of noise.

D. Real data

We here consider the sunspot data [3] used with OP in [25] as an illustrative example. Figure 6a shows the sunspot number $N = 3271$ of the months between year 1749 and 2021. Figure 6b shows obtained results using LPPE and classical PE applied to the full data samples. The LPPE oscillates between 0.39

and 0.82 and it reaches its maximum at L=79 months and its minimum at 273 months. We also divide the time series in 2 parts: years 1749-1900 and years 1901-2021, and we notice from fig.6c, 6d and 6e a difference in the complexity between both parts.

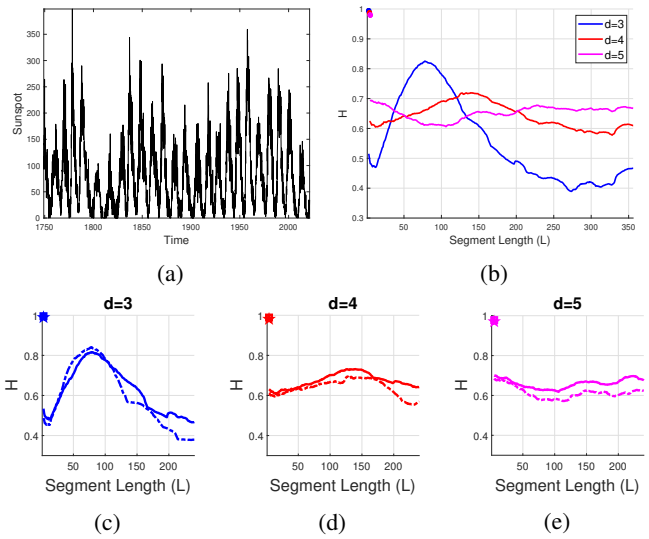

Fig. 6: LPPE applied to sunspot data. (a) Sunspot numbers from years 1749-2021 and (b) LPPE using d=3,4 and 5. (Solid circle) classical PE obtained using the same d. (c), (d) and (e) (-) LPPE of sunspot data for years 1479-1900 superimposed to (:) that of years 1901-2021.

V. Conclusions

In this paper, we introduce a new variant of MPE, named local Legendre polynomial modeling-based Permutation Entropy (LPPE). The aim is to benefit from the practical and theoretical relevance of polynomial approximation to form ordinal patterns of low order, using more sample data for a more accurate representation. This not only reduces computational costs but also overcomes the limitations of previously published MPEs. The proposed MPE benefits from the uncoupled model parameters due to the orthonormality property of Legendre polynomials. Furthermore, it is able to capture the growth rate of signals that were previously ignored in most traditional MPEs. The results obtained show that this new MPE is more robust against noise and less sensitive to sampling frequency than traditional MPE. Additionally, it facilitates the interpretation of PE-based complexity measures of real-data signals.

References

[1] C. E. Shannon, "A math. theory of communication," *The Bell System Technical Journal*, vol. 27, no. 3, pp. 379–423, 1948.

[2] A. M. Lyapunov, "The general problem of the stability of motion," *Intern. Journal of Control*, vol. 55, no. 3, pp. 531–534, 1992.

[3] G. Consolini, R. Tozzi, and P. De Michelis, "Complexity in the sunspot cycle," *Astronomy & Astrophysics*, vol. 506, no. 3, pp. 1381–1391, Nov. 2009.

[4] C. Bandt, "Order patterns, their variation and change points in financial time series and Brownian motion," *Statistical Papers*, vol. 61, no. 4, pp. 1565–1588, Aug. 2020.

[5] X. Huang, H. L. Shang, and D. Pitt, "A model sufficiency test using permutation entropy," *Journal of Forecast.*, Jan. 2022.

[6] M. Zanin, L. Zunino, O. A. Rosso, and D. Papo, "Permutation Entropy and Its Main Biomedical and Econophysics Applications: A Review," *Entropy*, vol. 14, no. 8, pp. 1553–1577, Aug. 2012.

[7] C. Bandt and B. Pompe, "Permutation Entropy: A Natural Complexity Measure for Time Series," *Physical Review Letters*, vol. 88, no. 17, p. 174102, Apr. 2002.

[8] W. Aziz and M. Arif, "Multiscale Permutation Entropy of Physiological Time Series," in *2005 Pakistan Section Multitopic Conference*, Dec. 2005, pp. 1–6.

[9] S.-D. Wu, C.-W. Wu, K.-Y. Lee, and S.-G. Lin, "Modified multiscale entropy for short-term time series analysis," *Physica A: Stat. Mechanics and its Applications*, vol. 392, no. 23, pp. 5865–5873, Dec. 2013.

[10] A. Humeau-Heurtier, C.-W. Wu, and S.-D. Wu, "Refined Composite Multiscale Permutation Entropy to Overcome Multiscale Permutation Entropy Length Dependence," *IEEE Signal Processing Letters*, vol. 22, no. 12, pp. 2364–2367, Dec. 2015.

[11] T. Liu, W. Yao, M. Wu, Z. Shi, J. Wang, and X. Ning, "Multiscale permutation entropy analysis of electrocardiogram," *Physica A: Stat. Mechanics and its Applications*, vol. 471, pp. 492–498, Apr. 2017.

[12] N. Qiao, L.-h. Wang, Q.-y. Liu, and H.-q. Zhai, "Multi-scale eigenvalues Empirical Mode Decomposition for geomagnetic signal filtering," *Measurement*, vol. 146, pp. 885–891, Nov. 2019.

[13] A. Davalos, M. Jabloun, P. Ravier, and O. Buttelli, "Multiscale Permutation Entropy: Statistical Characterization on Autoregressive and Moving Average Processes," in *2019 27th European Signal Processing Conference (EUSIPCO)*. A Coruna, Spain: IEEE, Sep. 2019, pp. 1–5.

[14] C. Morel and A. Humeau-Heurtier, "Multiscale permutation entropy for two-dimensional patterns," *Pattern Recognition Letters*, vol. 150, pp. 139–146, Oct. 2021.

[15] P. Ravier, A. Dávalos, M. Jabloun, and O. Buttelli, "The Refined Composite Downsampling Permutation Entropy Is a Relevant Tool in the Muscle Fatigue Study Using sEMG Signals," *Entropy*, vol. 23, no. 12, p. 1655, Dec. 2021.

[16] E. Olofsen, J. Sleigh, and A. Dahan, "Permutation entropy of the electroencephalogram: a measure of anaesthetic drug effect," *British Journal of Anaesthesia*, vol. 101, no. 6, pp. 810–821, Dec. 2008.

[17] J. F. Valencia, A. Porta, M. Vallverdu, F. Claria, R. Baranowski, E. Orlowska-Baranowska, and P. Caminal, "Refined Multiscale Entropy: Application to 24-h Holter Recordings of Heart Period Variability in Healthy and Aortic Stenosis Subjects," *IEEE Trans. on Biomed. Eng.*, vol. 56, no. 9, pp. 2202–2213, Sep. 2009.

[18] S. Berger, G. Schneider, E. F. Kochs, and D. Jordan, "Permutation entropy: Too complex a measure for EEG time series?" *Entropy*, vol. 19, no. 12, 2017.

[19] M. Jabloun, P. Ravier, and O. Buttelli, "On the Genuine Relevance of the Data-Driven Signal Decomposition-Based Multiscale Permutation Entropy," *Entropy*, vol. 24, no. 10, p. 1343, Sep. 2022.

[20] H. Azami and J. Escudero, "Amplitude-aware permutation entropy: Illustration in spike detection and signal segmentation," *Computer Methods and Programs in Biomed.*, vol. 128, pp. 40–51, 2016.

[21] Y. Chen, T. Zhang, W. Zhao, Z. Luo, and H. Lin, "Rotating machinery fault diagnosis based on improved multiscale amplitude-aware permutation entropy and multiclass relevance vector machine," *Sensors*, vol. 19, no. 20, 2019.

[22] L. Wan, G. Ling, Z.-H. Guan, Q. Fan, and Y.-H. Tong, "Fractional multiscale phase permutation entropy for quantifying the complexity of nonlinear time series," *Physica A: Stat. Mechanics and its Applications*, vol. 600, p. 127506, Aug. 2022.

[23] A. Dávalos, M. Jabloun, P. Ravier, and O. Buttelli, "On the Statistical Properties of Multiscale Permutation Entropy: Characterization of the Estimator's Variance," *Entropy*, vol. 21, no. 5, p. 450, Apr. 2019.

[24] M. Jabloun, "Empirical mode decomposition revisited using ordinal pattern concepts," in *2022 30th European Signal Proc. Conf. (EUSIPCO)*. Belgrade, Serbia: IEEE, 2022, pp. 2186–2190.

[25] C. Bandt and F. Shiha, "Order Patterns in Time Series," *Journal of Time Series Analysis*, vol. 28, no. 5, pp. 646–665, Sep. 2007.